ELECTRON EXCITATION CROSS SECTIONS FOR THE $3s^2 3p^2\ ^3P \rightarrow 3s3p^3\ ^5S^\circ$ TRANSITION IN S^{2+}

J. B. Greenwood, S. J. Smith, and A. Chutjian

Jet Propulsion Laboratory, California Institute of Technology, Pasadena, CA 91109

and

S. S. Tayal

Department of Physics, Clark Atlanta University, Atlanta, GA 30314

ABSTRACT

Experimental and theoretical collisional excitation cross sections are reported for the $3s^2 3p^2\ ^3P \rightarrow 3s3p^3\ ^5S^\circ$ spin-forbidden transition in S^{2+}. The transition energy (wavelength) is 7.33 eV (1691 Å). In the experimental approach, use is made of the electron energy-loss method with merged electron and ion beams. The metastable fraction in the S^{2+} beam is assessed and minimized. A novel "electronic aperture" is used to limit the trajectories of elastically-scattered electrons into the trochoidal electrostatic analyzer. Theoretically, the ***R***-matrix method in a 17-state and a 27-state calculation is used to obtain cross sections from threshold to 13.0 eV. Good agreement is found between experiment and the results of the 27-state theory. The presence of two strong resonances near threshold (7.5-8.5 eV) and a third resonance above threshold (11.5 eV) is verified by experiment.

Subject heading: atomic data – atomic processes

1. INTRODUCTION

Multiply-charged ions of sulfur and oxygen are present in the Io torus as a result of the volcanic activity at Io and the trapping effect of the Jovian magnetosphere. The S^{2+} ion is one of the more prominent emitters in the Io torus. Its transitions have been detected in the UV and VUV wavelength ranges by the *Hubble Space Telescope* (McGrath et al 1995), the *Hopkins Ultraviolet Telescope* (Hall et al 1994a), the *Extreme Ultraviolet Explorer* (Hall et al 1994b, Gladstone & Hall 1998), and *Voyager 1* (Taylor et al 1995). Its spin-forbidden $3s^23p^2\ ^3P \rightarrow 3s3p^3\ ^5S^\circ$ ($\lambda\lambda$1713,1719Å) transition has been used to calculate ion partitioning, and its intensity serves as one of many temperature diagnostics involving the species S^+, S^{2+}, and S^{3+} (Hall et al 1994a, Herbert & Hall 1998). The diagnostics are hampered by line blending and the lack of electron impact excitation rates for the observed transitions (Hall et al 1994b).

The present work is part of an ongoing effort to measure, and to compare with theory, absolute excitation cross sections for the ions which are important emitters in the Io torus. Data have been presented previously for O^+ (Zuo et al 1995) and S^+ (Liao et al 1997). Future work will include measurements on transitions in O^{2+} and S^{3+}. Measurements are made using the energy-loss, merged beams method, and the energy range is typically threshold to approximately 1.5-3 times threshold. A description of the experiment, and details unique to the e-S^{2+} measurements are given in § *2*. The theoretical ***R***-matrix approach is described in § *3*. Experimental results and results of the theoretical calculations are given in § *4*.

2. EXPERIMENTAL METHODS

Experiments were carried out using the JPL electron energy-loss, merged-beams facility with its 14.0 GHz electron cyclotron resonance ion source (ECRIS). The overall capabilities of the source with results have been described in a recent summary (Chutjian et al. 1999). Data acquisition and analysis methods have been described in work on e-C^{3+} excitation (Greenwood et al. 1999). A schematic diagram of the energy-loss facility may be found in Smith et al. (1999). Briefly, a beam of S^{2+} ions is derived from the ECRIS at an extraction voltage of 7 keV, or at a beam energy of 7q keV = 14 keV (an energy of 21 keV was used in the previous C^{3+} case). Carbon disulfide (CS_2) was used as the feed gas, with no other supporting gas used. The S^{2+} ions are mass/charge analyzed in a double-focusing 90° bending magnet. The beam is focused into the center of the interaction region through a series of baffled, differential-pumping regions and lens systems. The beam then interacts with a magnetically-confined electron beam which is merged with the ions through a trochoidal analyzer. The electrons and ions interact along a 20.0 $\pm$0.3 cm path length. The electrons are then de-merged from the ions using a second trochoidal analyzer. Detection is by means of a position-sensitive detector at the exit of the second trochoidal system. Beam profiles are measured at four locations along the merged path using vanes with slotted holes that intersect the merged beams at different radial distances. Discrimination against elastically-scattered electrons is through an electronic aperture which selectively filters electrons with large Larmor radii (predominantly the elastic ones) prior to the trochoidal analyzer, and through the use of retarding grids after the analyzer. Any remaining

elastically-scattered electrons which can overlap the inelastic spectrum are accounted for (and subtracted) through the use of trajectory modeling and calculated elastic differential cross sections. These three features, combined with the velocity-dispersion of the trochoidal monochromator, allow one to carry out measurements at energies both at, and significantly above, threshold.

The relation between the experimentally-measured quantities and the cross section $\sigma(E)$ (cm^2) for excitation at center-of-mass (CM) energy E is given by

$$\sigma(E) = \frac{\mathbb{R} q e^2 \mathcal{F}}{\epsilon I_i I_e L} \left| \frac{v_e v_i}{v_e - v_i} \right| , \qquad (1)$$

where $\mathbb{R}$ is the total signal rate (s^{-1}), q is the ionic charge state, e is the electron charge (C), I_e and I_i are the electron and ion currents (A) respectively, v_e and v_i are the electron and ion velocities (cm s^{-1}) respectively, L is the merged path length (cm), ϵ is the efficiency of the rejection grids/microchannel-plate detection system (dimensionless), and $\mathcal{F}$ is the overlap factor between the electron and ion beams (cm^2). All quantities in equation (1) are measured, or in the case of the particle velocities are known nominally through their acceleration potentials.

If we denote the laboratory energies of the electrons and ions as E_e and E_i, and their masses as m_e and m_i, respectively, expression for the CM energy E in equation (1), in terms of the laboratory (LAB) energies, is just

$$E = \mu\left[\frac{E_e}{m_e} + \frac{E_i}{m_i} - 2\left(\frac{E_e E_i}{m_e m_i}\right)^{1/2}\cos\vartheta\right] , \qquad (2)$$

where ϑ is the laboratory angle between the electron and ion beams. In addition to showing the energetics of the scattering, equation (2) is useful for calculating the expected behavior of the CM *resolution*, especially as a function of the laboratory electron energy E_e. This effect will be used in § *3* to discuss the experimental resolution of the sharp resonance structure observed in the S^{2+} excitation cross section near threshold. To demonstrate the behavior of resolution one may take the partial derivative of equation (1) with respect to E_e to obtain (after setting $\mu \sim m_e$),

$$\frac{\partial E}{\partial E_e} = 1 - \left(\frac{m_e}{m_i}\right)^{1/2}\left(\frac{E_i}{E_e}\right)^{1/2}\cos\vartheta . \qquad (3)$$

One can simplify this expression by taking $\vartheta \approx 0°$ (merged beams) so that, in terms of finite variations, one has

$$\Delta E = \Delta E_e\left[1 - 4.0187\times10^{-3}\left(\frac{E_i}{E_e}\right)^{1/2}\right] . \qquad (4)$$

The numerical coefficient within the brackets was calculated for a $^{34}S^{2+}$ ion at an energy of 14.0 keV. The variation of the CM energy resolution as a function of incident LAB electron energy E_e described by equation (4) is shown in Figure 1 for various choices of electron-energy resolution ΔE_e. The resolution is best at threshold, and approaches the limit ΔE_e for large E_e. As will be shown in § *3* this expression is useful for discussing

heights and widths of resonances which may be at various energies above threshold.

3. COLLISION CALCULATIONS

Included in the 27-state, ***R***-matrix close-coupling expansion were the LS-coupled S^{2+} states $3s^23p^2\ ^3P,^1D,^1S$; $3s3p^3\ ^{3,5}S^o,^{1,3}D^o,^{1,3}P^o$; $3s^23p3d\ ^{1,3}P^o,^{1,3}D^o,^{1,3}F^o$; $3s^23p4s\ ^{1,3}P^o$; $3s^23p4p\ ^{1,3}S,^{1,3}P,^{1,3}D$; $3s^23p4d\ ^{1,3}P^o,\ ^{1,3}D^o$. Thirteen orthogonal one-electron orbitals 1s, 2s, 2p, 3s, 3p, 3d, 4s, 4p, 4d, 4f, 5s, 5p, and 5d were used in the scattering calculation. The 1s, 2s, 2p, 3s, and 3p radial functions were chosen as the Hartree-Fock (HF) functions of the $3s^23p^2\ ^3P$ ground state of S^{2+} given by Clementi and Roetti (1974). The radial functions 3d, 4s, 4p, 4d, 4f, 5s, 5p, and 5d were chosen to give the best overall representation of the energies and oscillator strengths between states. Details of the wave functions are given by Tayal (1995, 1997a). Only the essential features are presented here. Included in the 17-state ***R***-matrix close-coupling expansion were the LS-coupled states $3s^23p^2\ ^3P,^1D,^1S$; $3s3p^3\ ^{3,5}S^o,^{1,3}D^o,^{1,3}P^o$; $3s^23p3d\ ^{1,3}P^o,^{1,3}D^o,^{1,3}F^o$; $3s^23p4s\ ^{1,3}P^o$.

The convergence of the configuration-interaction (CI) expansions is tested by considering up to two electron excitation from the basic configurations $3s^23p^2$, $3s3p^3$, $3s^23p3d$, $3s^23p4s$, $3s^23p4p$, and $3s^23p4d$. In the final calculation configurations with weights less than 0.005 were omitted and the 27 LS states were represented by 478 configurations. The optimized parameters of the radial functions, calculated excitation energies, and oscillator strengths of dipole-allowed and intercombination transitions can

be found in Tayal (1995, 1997a). It may be noted that Tayal (1997a) did not consider the 5d radial function in that 17-state calculation. It is necessary to include the 5d orbital to accurately represent the states of the $3s^2 3p4d$ configuration which are considered in the present 27-state calculation.

The total wave function representing the scattering of electrons by S^{2+} is expanded in the inner region ($r \leq a$) in the ***R***-matrix basis as (Berrington *et al.*, 1987)

$$\Psi_k = A\sum_{ij} c_{ijk}\bar{\Phi}(1,2,...,14;r_{15},\sigma_{15})u_{ij}(r_{15}) + \\ + \sum_j d_{jk}\phi_j(1,2,...,15) , \qquad (5)$$

where the functions Φ are formed by coupling the multiconfigurational functions Φ_i of the target bound states with the spin-angle functions of the scattered electron, and the u_{ij} are the numerical basis functions for the scattered electron. The operator A antisymmetrizes the wave function, and c_{ijk} and d_{jk} are expansion coefficients determined by diagonalizing the (N+1)-electron Hamiltonian.

The functions ϕ_j are of bound-state type and are included to compensate for the imposition of orthogonality conditions. Additional functions ϕ_j are included to allow for the short-range electron correlation effects. A total of 25 continuum orbitals in each channel were included which give good convergence for energies up to 9 Ry. Application of a variational principle led to a set of coupled integrodifferential equations which were solved numerically by the use of the ***R***-matrix method. The diagonal

elements of the inner-region Hamiltonian matrix are adjusted before diagonalization to reproduce observed energies of the target states.

The LS coupled ***K***-matrices were calculated using the Opacity ***R***-matrix computer codes (Berrington *et al.*, 1987) and by including mass correction and Darwin terms in the Hamiltonian. It should be noted that these relativistic effects do not give rise to fine structure splittings. A fine energy mesh of 0.002 Ry was chosen in the threshold region. The cross sections were calculated at 821 energy points to fully account for the narrow resonance structures. The ***R***-matrix calculation was carried out for partial waves with L=0 to 14, sufficient to obtain converged cross sections for the $3s^2 3p^2\ ^3P \rightarrow 3s3p^3\ ^5S^o$ transition considered in the present work.

4. RESULTS AND DISCUSSION

The (unconvoluted) theoretical results of the 17-state and 27-state ***R***-matrix calculations are shown in Figure 2. The presence of many sharp resonance structures is evident. In particular, several of the resonances appear to be broad relative to the energy resolution in the experiments (Figure 1), and hence can be resolved.

Experimental results are shown in Figure 3, where the data are displayed separately for the 17-state and 27-state results. Results in both theoretical calculations have been folded with a 100 meV (FWHM, LAB) Gaussian electron energy distribution function, with the variation shown in Figure 1. The experimental data are listed in Table

1 at the discrete energies of the experiment. Convoluted, theoretical data are not listed as a point-by-point comparison was not deemed meaningful.

Two strong resonances at threshold (7.5-8.5 eV) and a third broader resonance near 11.5 eV are clearly detected with the resolution of the measurements. Overall, the 27-state results give better agreement with experiment than results in the 17-state calculation. Experimental data show two clear resonance peaks near threshold, with evidence for smaller oscillations in the interval 8-9 eV. The 17-state calculation gives more oscillations in the 7-9 eV range. These oscillations either are not present in the experiment, or were not resolved due to either experimental resolution or insufficient step size in the data. Results of experiment and both theories agree on the energy position and width of the broad resonance at 11.5 eV.

ACKNOWLEDGMENTS

JBG thanks the National Research Council for a fellowship through the NASA-NRC program. SST was supported through NASA Grant NAG5-6889. The computational work was carried out on the JPL/Caltech Cray Supercomputer. Experimental measurements were carried out at JPL/Caltech through support of NASA.

REFERENCES

Berrington, K. A., Burke, P. G., Butler, K., Seaton, M. J., Storey, P. J., Taylor, K. T., & Yan, Y. 1987, J. Phys. B: Atom. Molec. Phys., 20, 6379

Clementi, E., & Roetti, C. 1974, At. Data Nucl. Data Tables, 14, 177

Chutjian, A., Greenwood, J. B., & Smith, S. J. 1999, in Applications of Accelerators in Research and Industry (eds. J. L. Duggan & I. L. Morgan, New York: AIP)

Gladstone, G. R., & Hall, D. T. 1998, J. Geophys. Res., 103, 19927

Greenwood, J. B., Smith, S. J., & Chutjian, A. 1999, Phys. Rev. A, 59, 1348

Hall, D. T., Bednar, C. J., Durrance, S. T., , Feldman, P. D., McGrath, M. A., Moos, H. W., & Strobel, D. F. 1994a, ApJ, L45

Hall, D. T., Gladstone, G. R., Moos, H. W., Bagenal, F., Clarke, J. T., Feldman, P. D., McGrath, M. A., Schenider, N. M., Shemansky, D. E., Strobel, D. F., & Waite, J. H. 1994b, ApJ, 426, L51

Herbert, F., & Hall, D. T. 1998, J. Geophys. Res., 103, 19915

Liao, C., Smith, S. J., Hitz, D., Chutjian, A., & Tayal, S. S. 1997, ApJ, 484, 979

McGrath, M. A., Hall, D. T., Matheson, P. L., Weaver, H. A., Trauger, J. T., Smith, T. E., Thomas, N., Gladstone, R., Schenider, N. M., Harris, W. M., Livengood, T. A., Prangé, R., & Festou, M. C. 1995, Science, 1313.

Tayal, S. S. 1997a, ApJ, 481, 550

Tayal, S. S. 1997b, At. Data Nucl. Data Tables, 67, 331

Tayal, S. S. 1995, J. Phys. B: Atom. Molec. Phys., 28, 5193

Taylor, M. H., Schneider, M. A., Bagenal, F., Sandel, B. R., Shemansky, D. E.,

Matheson, P. L., & Hall, D. T. 1995, J. Geophys. Res., 100, 19541

Zuo, M., Smith, S. J., Chutjian, A., Williams, I. D., Tayal, S. S., and McLaughlin, B. M. 1995, ApJ, 440, 421

TABLE 1

Experimental and Theoretical (***R***-Matrix) Cross Sections $\sigma(E)$ for the $3s^2 3p^2\ ^3P \rightarrow 3s3p^3\ ^5S^\circ$ spin-forbidden transition in S^{2+}.

Energy (eV)	Experimental $\sigma(E)$	Energy (eV)	Experimental $\sigma(E)$
7.07	0.03	8.88	0.17
7.22	0.07	8.89	0.66
7.35	0.27	8.91	0.99
7.48	0.52	8.99	0.44
7.55	0.59	9.07	0.47
7.65	1.32	9.07_1	0.46
7.76	1.61	9.37	0.38
7.84	0.99	9.45	0.32
7.92	1.06	9.75	0.26
8.05	0.67	10.2	0.31
8.14	0.41	10.3	0.46
8.22	0.75	10.5	0.29
8.31	0.61	10.6	0.32
8.41_7	0.71	10.9	0.55
8.42	0.48	11.0	0.69
8.44	0.56	11.2	0.71
8.51	0.59	11.3	0.89
8.52	0.62	11.4	0.85
8.62	0.99	11.5	1.20
8.67	0.29	11.5_6	1.24

8.67_4	1.11	11.6_4	1.09
8.74	0.65	11.7	0.70
8.76	0.55	11.9	0.81
8.77	0.96	12.1	0.74
8.78	1.30		

NOTES.–Theoretical results have been convoluted with a CM-corrected eV (FWHM) Gaussian electron energy width (see Fig. 1). Units of cross section are 10^{-16} cm^2.

[a]Nonzero values in experiment and theory below threshold include effects of the electron-energy spread in the experiment.

FIGURE CAPTIONS

Figure 1. – Calculated variation of the CM energy resolution ΔE with incident LAB electron energy E_e. Each curve is labeled by the resolution ΔE_e of the incident electron beam.

Figure 2. – Theoretical, unconvoluted 17-state (top) and 27-state (bottom) ***R***-matrix calculations for the $3s^2 3p^2\ ^3P \rightarrow 3s3p^3\ ^5S^\circ$ spin-forbidden transition in S^{2+}.

Figure 3. – Experimental results (filled circles) and results of theoretical ***R***-matrix calculations (solid line) for the $^3P \rightarrow ^5S^\circ$ transition in S^{2+}. Shown at the top is comparison with the 17-state ***R***-matrix calculation, and at the bottom with the 27-state calculation. Theoretical results have been convoluted with a constant Gaussian electron-energy width of 100 meV (FWHM).

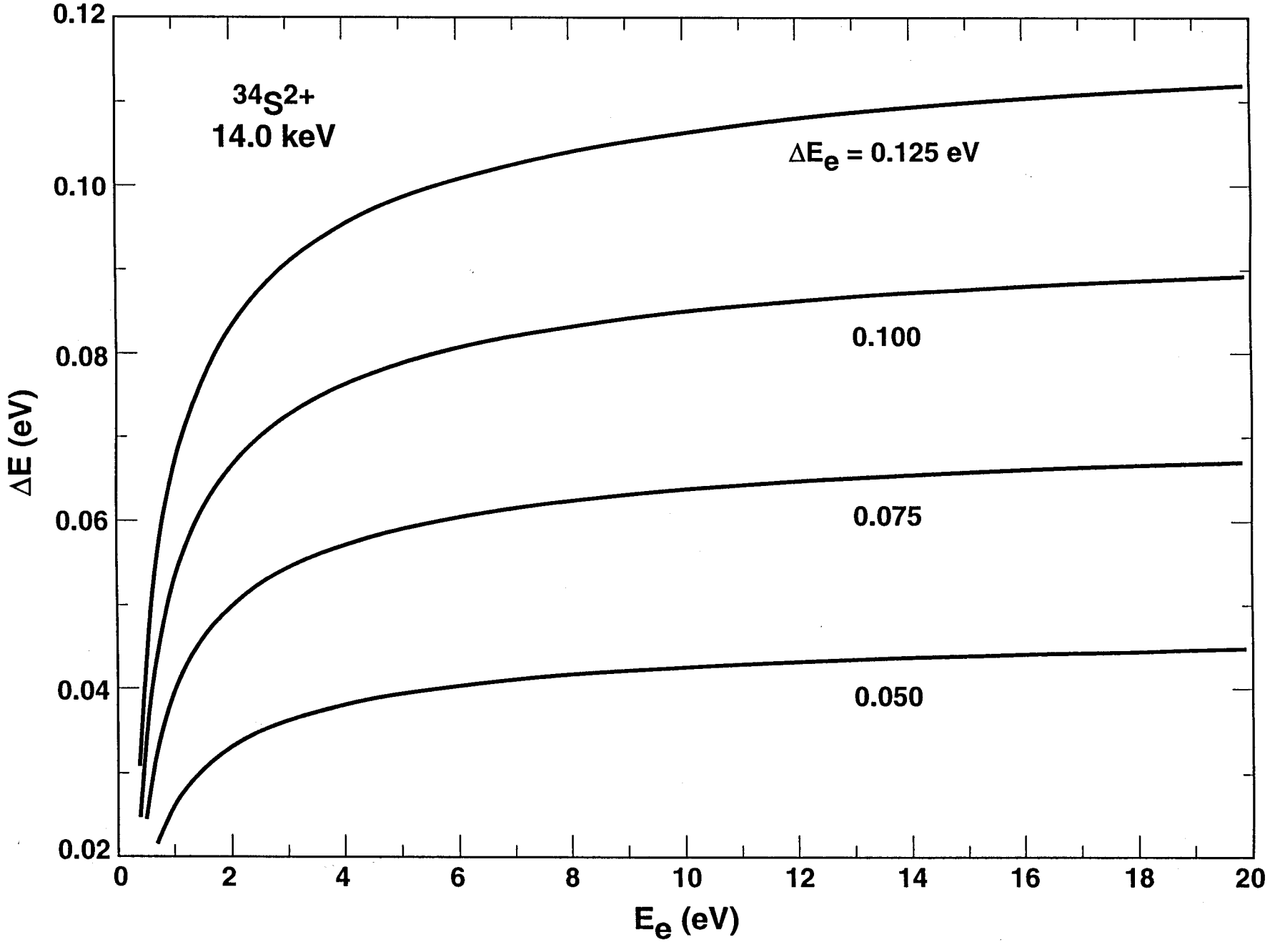
$^{34}S^{2+}$
14.0 keV
ΔE_e = 0.125 eV
0.100
0.075
0.050
0.12
0.10
0.08
0.06
0.04
0.02
ΔE (eV)
0
2
4
6
8
10
12
14
16
18
20
E_e (eV)

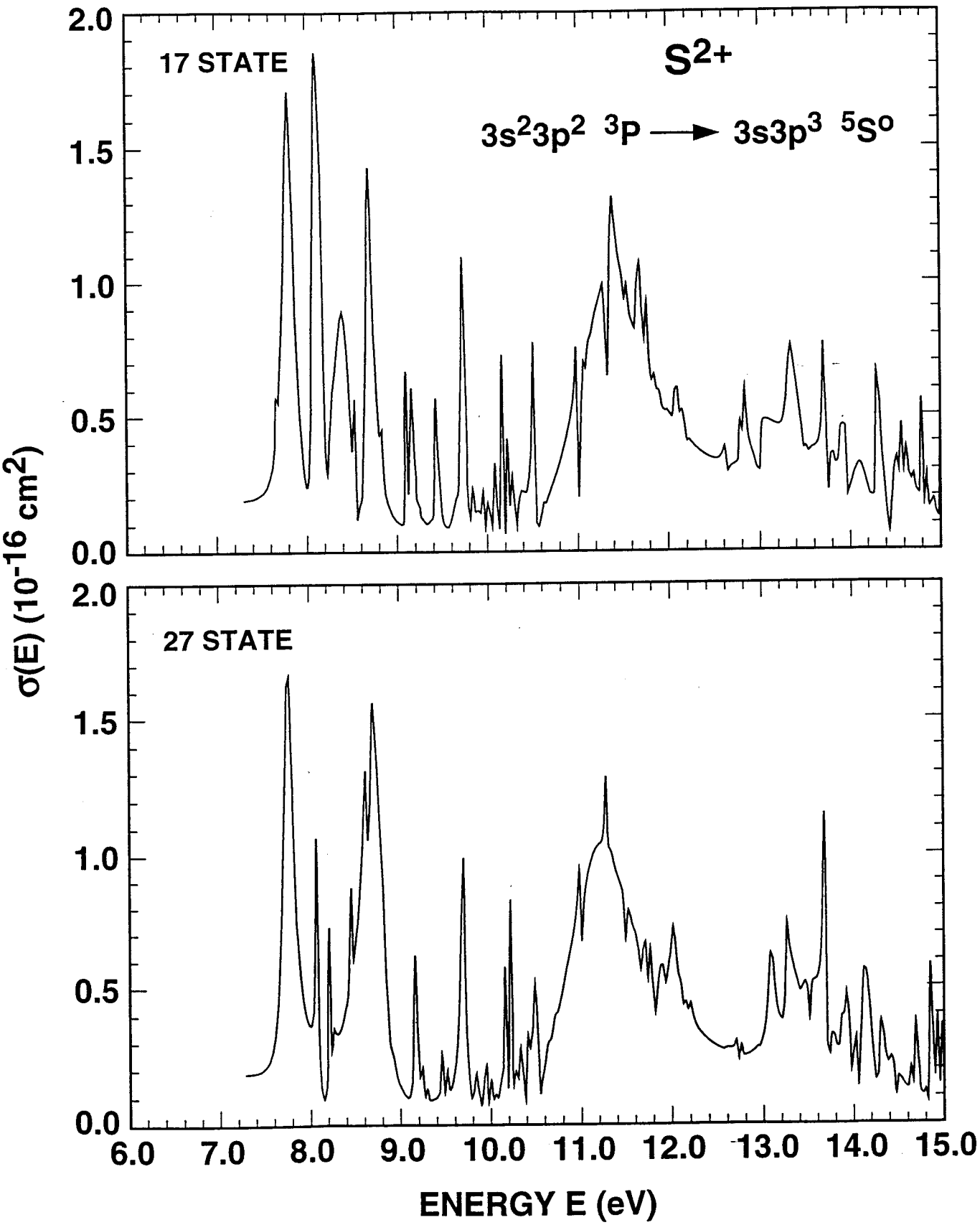
17 STATE
S^{2+}
$3s^23p^2\ {}^3P \longrightarrow 3s3p^3\ {}^5S^o$
27 STATE
$\sigma(E)\ (10^{-16}\ cm^2)$
ENERGY E (eV)
2.0
1.5
1.0
0.5
0.0
6.0
7.0
8.0
9.0
10.0
11.0
12.0
13.0
14.0
15.0

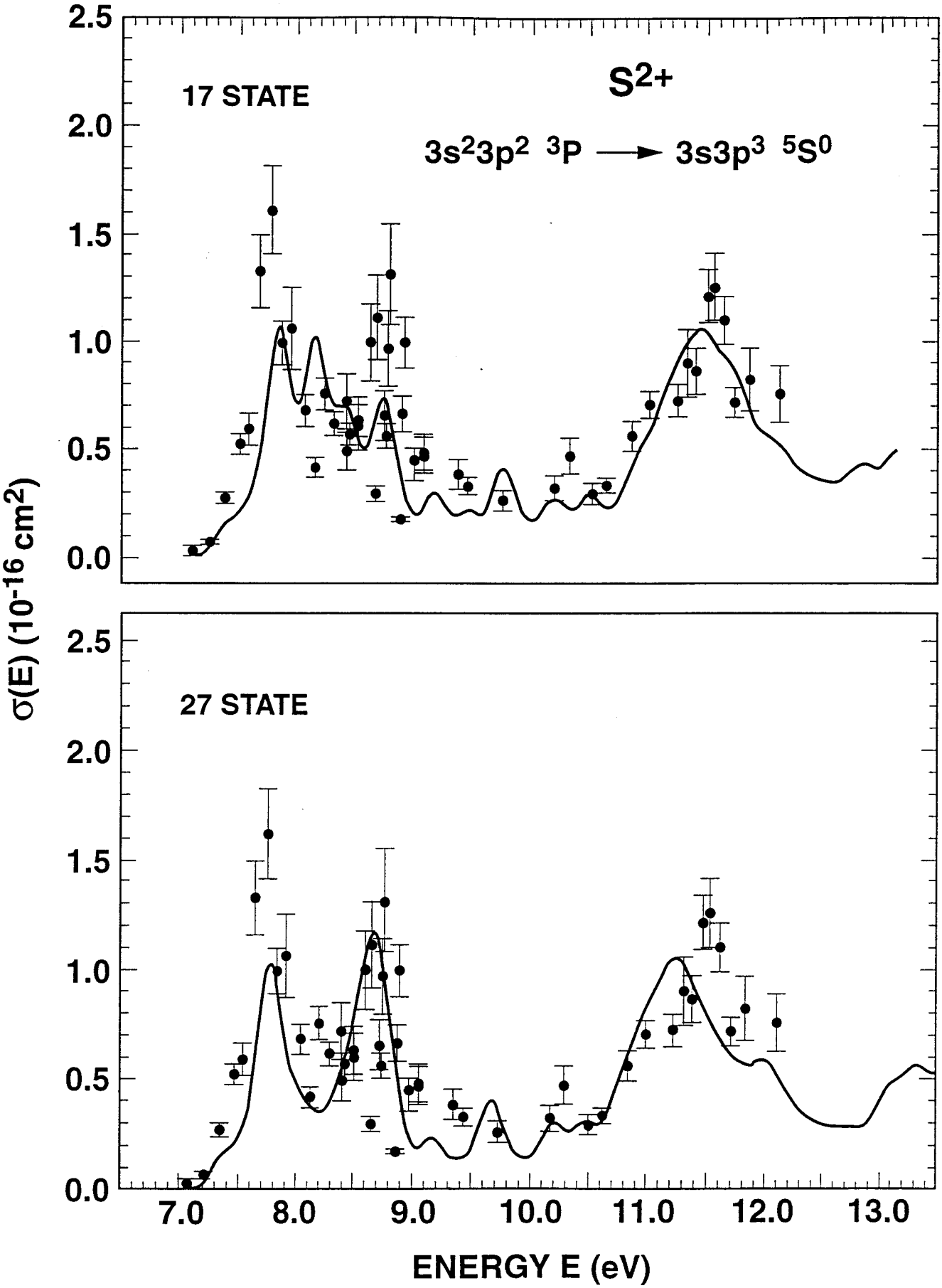
17 STATE
S^{2+}
$3s^23p^2\ ^3P \longrightarrow 3s3p^3\ ^5S^0$
27 STATE
$\sigma(E)\ (10^{-16}\ cm^2)$
ENERGY E (eV)
0.0
0.5
1.0
1.5
2.0
2.5
7.0
8.0
9.0
10.0
11.0
12.0
13.0